Science of the Total Environment 835 (2022) 155351

Contents lists available at ScienceDirect

Science of the Total Environment

journal homepage: www.elsevier.com/locate/scitotenv

Spatial heterogeneity in chemical composition and stability of glomalin-related soil protein in the coastal wetlands

Zhenli Guo [a], Jingchun Liu [a,*], Jiajia Wu [a], Dan Yang [c], Kang Mei [a,b], Hanyi Li [a], Haoliang Lu [a], Chongling Yan [a]

[a] Key Laboratory of Ministry of Education for Coastal and Wetland Ecosystems, Xiamen University, Xiamen 361102, China
[b] State Key Laboratory of Marine Environmental Science, Xiamen University, Xiamen 361102, China
[c] Key Laboratory of Plant Resource Conservation and Germplasm Innovation in Mountainous Region, Collaborative Innovation Center for Mountain Ecology & Agro-Bioengineering, College of Life Sciences, Guizhou University, Guiyang 550025, China

HIGHLIGHTS

- GRSP concentration in mangrove forest soil was significantly higher than that in the mudflat.
- The C/N ratio of GRSP increased with depth in the coastal wetlands.
- The chemical composition of GRSP could be an indicator for SOM heterogeneity.
- The stability of GRSP and its contribution to SOC increased with increasing depth.
- The deeper soil layers are more conducive for GRSP sequestration.

GRAPHICAL ABSTRACT

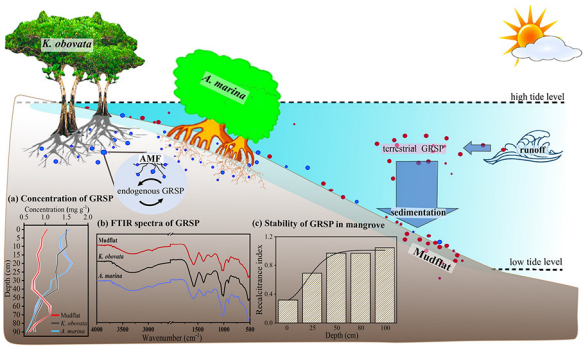

ARTICLE INFO

Editor: Jan Vymazal

Keywords:
Coastal ecosystem
GRSP
Infrared spectra
^{13}C NMR
Carbon sequestration

ABSTRACT

GRSP is widely distributed in coastal wetlands, and there is a tendency for it to degrade with increasing burial depth. However, the dynamic changes in the chemical composition and stability of GRSP during the burial process are still unclear. The purpose of this study is to clarify the chemical composition and accumulation characteristics of GRSP during the burial process in the Zhangjiang estuary. In a field study, soil cores to the depth of 100 cm were collected in the estuary from mangrove forests dominated by *Kandelia obovata* and *Avicennia marina*, and from mudflat. The results showed that the concentration of GRSP in mangrove forest soil was significantly higher than that in the mudflat ($p < 0.05$), and the C/N ratio of GRSP increased with depth at all sites. Analysis of Fourier transform infrared (FTIR) data showed that the degradation rates of the GRSP's compositions varied with increasing burial depth, with microbial action and pH possibly being the main factors affecting degradation. Values of recalcitrance index (RI) showed that the stability of GRSP increased with increasing depth, and the contribution of GRSP to soil organic carbon (SOC) also increased. This suggests that the burial process plays a role in screening and storing the stable components of GRSP. Overall, our findings suggest that the concentration and chemical composition of GRSP vary dynamically according to habitat and burial processes. In addition, the improved stability of GRSP could contribute to carbon sequestration in coastal wetlands.

1. Introduction

Glomalin-related soil protein (GRSP) is usually considered to be a refractory and thermostable glycoprotein produced by ubiquitous arbuscular mycorrhizal fungi (AMF) (Rillig, 2004; Driver et al., 2005; Rosier et al., 2008). Studies have proven that GRSP plays an important

* Corresponding author.
E-mail address: liujingchun@xmu.edu.cn (J. Liu).

http://dx.doi.org/10.1016/j.scitotenv.2022.155351
Received 28 December 2021; Received in revised form 6 April 2022; Accepted 13 April 2022
Available online 20 April 2022

role in reducing soil carbon dioxide emissions, promoting carbon storage (He et al., 2020), and enhancing plant resistance to environmental stress (Barea et al., 2014; Singh et al., 2016; Kumar et al., 2018). In addition, GRSP has important environmental functions in terms of promoting the formation of soil aggregates (Rillig et al., 2001), adsorbing heavy metals (Vodnik et al., 2008; Wang et al., 2020), and reducing the soil adsorption of organic chemicals (Chen et al., 2020). Studies have shown that GRSP is a complex mixture (Gillespie et al., 2011; Staunton et al., 2020) and its chemical composition could be modified by environmental factors (Schindler et al., 2007) such as vegetation types, soil physicochemical properties, microbial action, and human activities (Holátko et al., 2021). Differences in the chemical composition of GRSP may reflect different environmental functions. Therefore, this glycoprotein should be considered from a dynamic perspective. However, research into aspects of its chemical composition is still limited, preventing a more comprehensive understanding of GRSP and its possible ecological functions.

Coastal wetlands are located in the marine-terrestrial interlaced zone, which is a typically fragile and sensitive environment (Negrin et al., 2011; Yang et al., 2017; Xu et al., 2021). Wetlands are also important transmission channels for various materials and energy (Silva et al., 2007). For example, mangrove wetlands have been proven to represent a considerable carbon pool due to the high growth rate of plants, high sedimentation rates, and the presence of an anaerobic waterlogged soil environment (Liu et al., 2014). GRSP is one of the components of soil organic matter (SOM) (Singh et al., 2017; Xiao et al., 2019). It contributes as much as 3%–10% to soil carbon storage in mangroves (Lovelock et al., 2004a; Treseder et al., 2007), a level second only to that stored in tropical forest (Singh et al., 2017). For these reasons, coastal wetlands are ideal natural sites in which to investigate dynamic changes in the chemical composition of GRSP.

GRSP has been considered as a bioindicator of terrestrial-marine linkages (Adame et al., 2012). In mangrove forest soils, it can be classified as endogenous or terrestrial GRSP depending on its source. The former is produced by AMF in mangrove roots (Kothamasi et al., 2006), while the latter is produced in terrestrial ecosystems and is transported to coastal wetlands by runoff (Tian et al., 2020). Furthermore, mangrove areas have high sedimentation rates. Knowledge of the transformation processes of organic carbon during burial is essential if soil carbon pool dynamics are to be understood (Chaopricha and Marín-Spiotta, 2014). Several studies have shown that the concentration of GRSP decreases with increasing burial depth (Wu et al., 2012; Wang et al., 2019; Das et al., 2020). However, it is still unknown whether or not the chemical composition of GRSP varies during the burial process, and how this may occur. Additionally, the relative stability of GRSP means that its accumulation rate in soil usually higher than that of other SOM components (Zhang et al., 2015; Jia et al., 2016), which is an important factor in its carbon sequestration potential. Nevertheless, information on the variation in its stability during burial in coastal wetland soils is still scarce. It is therefore necessary to clarify the effects of the burial process on the chemical composition and stability of GRSP.

Our objectives were to assess the effects of habitat differences and burial processes on the chemical composition and stability of GRSP in coastal mangrove forest and mudflat. We collected soil cores at depths of 0–100 cm and determined the soil's physicochemical properties (pH, SOC, SOM-C/N, GRSP concentration). We also characterized the chemical composition and stability of GRSP using FTIR and solid-state ^{13}C NMR technology. Based on previous reports of differences in GRSP concentration in various coastal wetland habitats (Tian et al., 2020; Wang et al., 2018), we hypothesized that there may also be differences in its chemical composition due to different plant types, soil physicochemical properties, and tidal levels. Moreover, we expected that GRSP chemical composition could also change due to root interaction and changes in the soil environment during burial processes. We also intended to clarify the trends in GRSP stability with increasing burial depth and its contribution to carbon storage in mangrove wetlands.

2. Materials and methods

2.1. Study area

The study area is located in the Zhangjiang Estuary Mangrove National Nature Reserves (ZEMNNR) (23°55′ N, 117°30′ E), Fujian Province, China (Fig. 1). It has a subtropical maritime monsoon climate, with an average annual temperature of 21.2 °C and an annual average precipitation of 1714.5 mm. Tides are irregular and semi-diurnal, with an average tidal range of 2.32 m (Zhang et al., 2012; Feng et al., 2017), and the salinity of the seawater is 12‰–26‰. The dominant plant species in the study area are *Kandelia obovata* (*K. obovata*), *Avicennia marina* (*A. marina*), and *Aegiceras corniculatum* (*A. corniculatum*).

2.2. Soil collection and preparation

Three sampling sites were selected from low to high tide levels. They were respectively located at mudflat (low tidal level; salinity = 20.17 ± 2.51‰), pure *A. marina* mangrove forest (medium tidal level; salinity = 15.97 ± 1.04‰; average tree height = 2.32 ± 0.24 m, and branch diameter = 11.78 ± 3.62 cm), and pure *K. obovata* mangrove forest (high tidal level; salinity = 13.86 ± 1.33‰; average tree height = 2.53 ± 0.23 m, and branch diameter = 12.21 ± 3.16 cm). Each core was collected with a drill bit extractor at each sampling site on August 6, 2020 during the low tidal period (Fig. 1).

As soon as the cores were taken, they were layered with a plastic cutter and immediately sealed in plastic zip-lock bags. According to the intensity of root action in mangrove forest soils, we divided the soil core into the root action zone (0–30 cm) and non-root action zone (30–100 cm). The mudflat soil core was divided in the same way. Soil cores from the root zone (0–30 cm) were divided at 5 cm intervals (0–5 cm, 5–10 cm, 10–15 cm, 15–20 cm, 20–25 cm, and 25–30 cm), and those cores in the non-root zone (30–100 cm) were divided at 10 cm intervals (30–40 cm, 40–50 cm, 50–60 cm, 60–70 cm, 70–80 cm, 80–90 cm and 90–100 cm). Each core was divided into 13 sub-samples, giving 39 sub-samples in total. After sealing, the sub-samples were stored in an icebox and immediately transferred to the laboratory where they were dried in a freeze dryer. After removing branches, shells, and other large impurities, the dried soil samples were ground up for later analysis.

2.3. Determination of soil physicochemical properties

Soil samples were firstly sieved using a 2 mm nylon sieve and the soil pH was measured in soil-water suspension (1:5) using a pH meter (PHS-2F). The samples were then sieved to 0.149 mm. Values of soil organic matter-C/N (SOM-C/N) were determined using a Vario EL Cube Element Analyzer (Elementar, Germany) after hydrochloric acid pretreatment to remove inorganic carbon from the dried soil. The procedure was as follows: 0.5 g of each soil sample was taken and dipped in 1 mol L^{-1} HCl in a 50 mL centrifuge tube, removing the supernatant after the bubbles disappeared. The centrifuge tubes containing acidified soil were dried in a drying oven at 60 °C for 48 h. The dried soil samples were ground again and sieved to 0.149 mm for testing. The acid-treated and dried soil samples were wrapped in tin capsules, and the value of SOM-C/N was determined using the elemental analyzer.

2.4. GRSP extraction, determination, and purification

The soil samples were sieved to 0.25 mm and used for GRSP extraction. The total GRSP (T-GRSP) was extracted by autoclaving triplicate samples in 50 mM sodium citrate solution (pH = 8; soil:solution ratio = 1:8 g mL^{-1}) for 60 min at 121 °C. Each gram of soil sample was extracted 3 times until the reddish-brown colour in the supernatant faded. The supernatants obtained after centrifuging at 8000 × *g* for 10 min were stored at 4 °C for further analysis, while the easily-extracted GRSP (EE-GRSP) was extracted in 20 mM sodium citrate solution (pH 7; soil:solution ratio = 1:8 g mL^{-1})

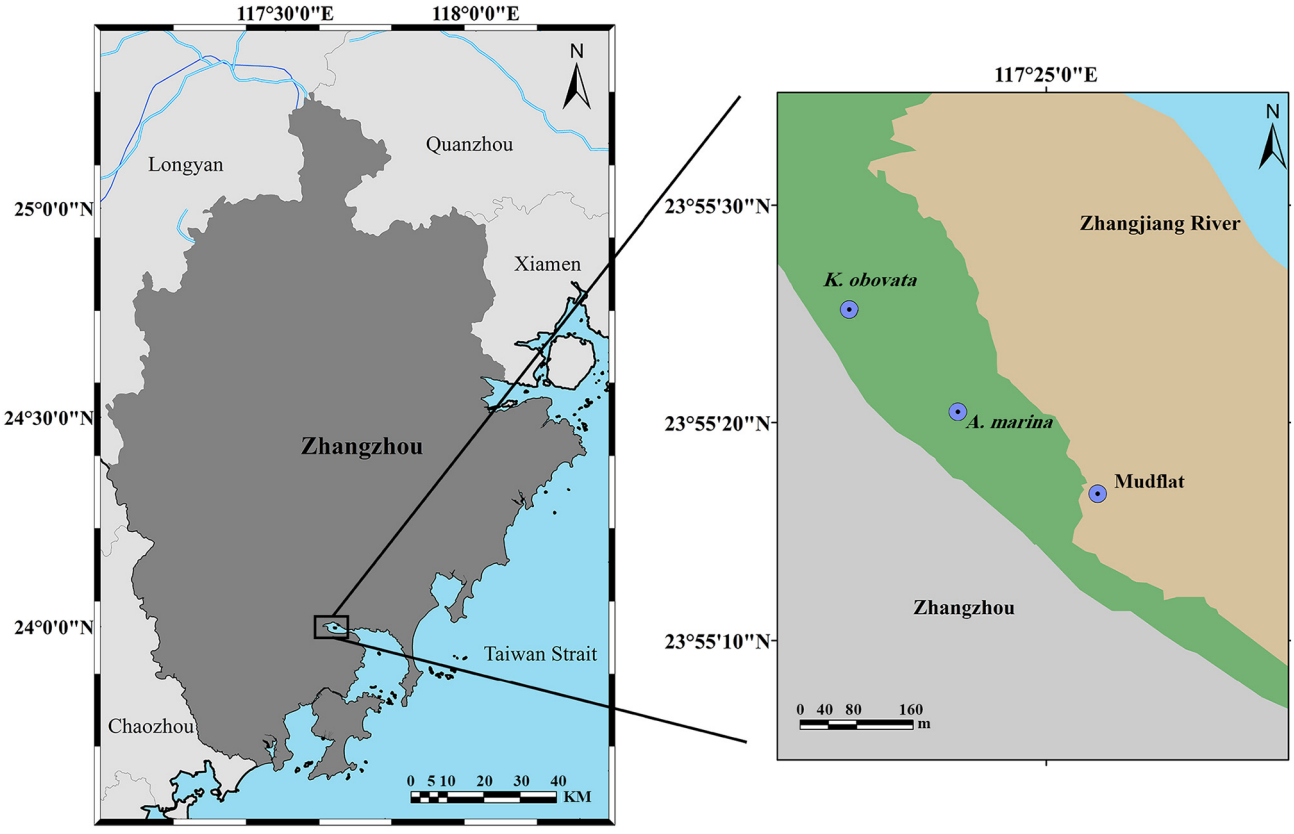

Fig. 1. Geographical location map of sampling sites. The sampling sites are located in Zhangjiang Mangrove Reserve, Zhangzhou City, China. The mudflat site is located at low tidal level with no vegetation growth. The sampling site of *A. marina* mangrove forest is located at the medium tidal level, and the sampling site of *K. obovata* mangrove forest is located at the high tidal level. The linear distances of the three sampling points are all above 100 m.

for 30 min at 121 °C. The supernatants obtained after centrifuging at 4000 $\times g$ for 8 min were then stored at 4 °C for further analysis (Zhang et al., 2014; Zhu et al., 2019). The T-GRSP and EE-GRSP concentrations were determined using Bradford's dye-binding assay, employing bovine serum albumin (BSA) as the standard (Wright and Upadhyaya, 1998).

The specific steps of the purification of GRSP are as follows: the extracted T-GRSP solution was adjusted to pH 2.0 with 1 mol L^{-1} HCl to precipitate GRSP. After placing in an ice bath for 24 h, it was centrifuged at 8000 $\times g$ for 10 min and the precipitate retained. Then 0.1 mol L^{-1} NaOH was added to the precipitate and the resulting solution was poured into a dialysis bag (DW = 8000–14,000 Da) which was placed in deionized water (dH_2O) for 18 h. The dH_2O was replaced every 6 h, three times in total. After the dialysate had been freeze-dried, the final dried floc was the purified GRSP (Gillespie et al., 2011). The C/N ratio of the purified GRSP was determined using the Vario El Cube Element Analyzer (Elementar, Germany).

2.5. Fourier transform infrared (FTIR) spectroscopy analysis

In this study, FTIR analysis was performed on nine purified GRSP samples. Six of the samples were extracted from the surface (0–5 cm) and bottom (90–100 cm) layers of the three soil cores, and the other three were extracted from the *K. obovata* mangrove forest soil core at depths of 25–30 cm, 50–60 cm, and 80–90 cm. The compositional traits of the purified GRSP from the three sample sites were determined using an attenuated total reflection Fourier transform infrared (ATR-FTIR) spectrometer (Bruker Vertex 70V, Germany) with a spectral range of 4000–500 cm^{-1}. The resolution of the instrument is greater than 0.40 cm^{-1} and its wavenumber accuracy is better than 0.01 cm^{-1}. The peak areas in the spectra were integrated using Origin 2018 software (Origin Lab Corporation, USA) to obtain semi-quantitative data for the characteristic compositions (Wang et al., 2014). The band partitioning method is described in Table S1.

2.6. Nuclear magnetic resonance (NMR) spectroscopy analysis

Solid-state variable amplitude cross-polarization magic angle spinning (SS (MAS) ^{13}C NMR) spectroscopic analysis was performed on five purified GRSP samples from *K. obovata* mangrove forest soil taken at depths of 5, 30, 60, 90, and 100 cm, in order to investigate variations in the carbon fraction and degradation of GRSP with increasing burial depth. Employing the method described by Schindler et al. (2007) and optimizing the parameters, the SS (MAS) ^{13}C NMR spectra of purified GRSP were obtained using a 600 MHz WB Solid-State Nuclear Magnetic Resonance Spectrometer (A Bruker AVANCE NEO, Switzerland). Samples were placed into a 3.2 mm CPMAS rotor and spun at 12 kHz at the magic angle. The acquisition conditions were set at a frequency rate of 150.9 MHz, with a spectra width of 45.5 kHz, single contact time of 2 ms, and recycle delay time of 3 s. Approximately 30,000 scans of purified GRSP were collected from each sample.

2.7. Data analysis

2.7.1. GRSP stability analysis

To investigate the effect of high deposition rate on the GRSP's stability in mangrove forests, stability analyses were performed on five purified GRSP samples from *K. obovata* mangrove forest taken at depths of 5, 30, 60, 90, and 100 cm. The GRSP enrichment factor can be used as an indicator of GRSP stability (Cissé et al., 2020), where an increase in the value of this factor means that GRSP concentration decreases more slowly than other SOM components. The enrichment factor is calculated as follows:

$$\text{Enrichment factor of GRSP} = \text{GRSP}/\text{SOC} \quad \text{(a)}$$

Meanwhile, the SS ^{13}C NMR spectra can be divided into four regions for the major carbon-containing functional groups (Table S2), and the concentration of the four kinds of carbon component can then be used as an indicator of the stability of GRSP as expressed by the recalcitrance index (RI) (Ostertag et al., 2008; Zhang et al., 2017). The alkyl and aromatic compounds include long-chain aliphatic compounds, tannins, waxes, cutin, suberin, and lignin, which are hydrophobic and resistant to decay (Table S2), while the O-alkyl and carboxyl C groups represent compounds such as hydrophilic and labile organic acids (Baldock et al., 1992; Ostertag et al., 2008). The recalcitrance index is calculated as follows:

$$RI = (\text{alkyl C} + \text{aromatic C})/(\text{O}-\text{alkyl C} + \text{carboxyl C}) \quad (b)$$

2.7.2. Statistical analysis

Three parallel samples were made for each sample. Before a significance analysis was conducted, normality was assessed using the Shapiro-Wilk test, and the homogeneity of variances was determined using Levene's test. Pearson correlation analysis was used to explore the correlation between the variables. One-way ANOVA was subsequently performed, followed by the least-significant difference (LSD) test for multiple comparisons at $p < 0.05$.

The test of significance using one-way ANOVA and the Pearson correlation analysis were performed with SPSS 25.0 statistical software (IBM Corporation, USA). All figures were plotted using Origin 2018 software (Origin Lab Corporation, USA), and the map of sample sites was drawn using ArcGIS 10.2 software (ESRI, USA).

3. Results

3.1. GRSP and SOC concentration

The vertical distribution of T-GRSP, EE-GRSP, and SOC concentrations in the three sampling sites are shown in Fig. 2. *K. obovata* mangrove forest soil had the highest concentrations of T-GRSP (1.16 ± 0.29 mg g^{-1}) and EE-GRSP (0.39 ± 0.07 mg g^{-1}), followed by the *A. marina* mangrove forest (1.13 ± 0.37 mg g^{-1} and 0.38 ± 0.13 mg g^{-1}, respectively), while the lowest concentrations were found in the mudflat (0.87 ± 0.15 mg g^{-1} and 0.29 ± 0.05 mg g^{-1}, respectively). T-GRSP and EE-GRSP concentrations decreased with increasing depth. Compared with the surface soil (5 cm), the concentration of T-GRSP and EE-GRSP at the bottom layer (100 cm) of the *K. obovata* mangrove forest soil core showed the highest decreases (64% and 63%, respectively), while lower decreases were found in the mudflat soil core (41% and 38%, respectively). EE-GRSP concentration did not fluctuate significantly with increasing depth, and decreases in EE-GRSP concentration were smaller than those of T-GRSP in all sites (Fig. 2). SOC concentration was highest in the *K. obovata* mangrove forest soil (17.60 ± 6.87 mg g^{-1}), followed by that in the *A. marina* mangrove forest (15.54 ± 4.22 mg g^{-1}), and the lowest in the mudflat (8.69 ± 0.95 mg g^{-1}) (Fig. 2).

There was a significant positive correlation between T-GRSP and SOC at the three sampling sites (*K. obovata* mangrove forest, $R^2 = 0.977$, $p < 0.05$; *A. marina* mangrove forest, $R^2 = 0.971$, $p < 0.05$; mudflat, $R^2 = 0.876$, $p < 0.05$). The one-way ANOVA showed that there was no significant difference in GRSP concentration between the two mangrove forest types in the root action zone (0–30 cm). However, T-GRSP concentration in the mangroves was significantly lower than that in the mudflat ($p < 0.05$) (Fig. 2). In the non-root action zone (30–100 cm), there was no significant difference in T-GRSP concentration among the three sampling sites ($p > 0.05$) (Fig. 2).

3.2. C/N ratios of GRSP, SOM, and soil

The vertical trends of SOM-C/N and GRSP-C/N in the soils collected at each site were found to be consistent (Fig. 3). The mean value of SOM-C/N varied from large to small as follows: *K. obovata* (13.21 ± 1.06 mg g^{-1}) > *A. marina* (11.61 ± 1.11 mg g^{-1}) > mudflat (10.83 ± 1.93 mg g^{-1}), while the mean value of GRSP-C/N also varied from large to small: mudflat (12.86 ± 4.45 mg g^{-1}) > *K. obovata* (11.72 ± 0.92 mg g^{-1}) > *A. marina* (10.86 ± 1.33 mg g^{-1}) (Fig. 3). Pearson correlation analysis showed that GRSP-C/N and SOM-C/N levels were positively correlated ($p < 0.05$) (Table S3).

Further analysis revealed that there was no significant difference in GRSP-C/N among the three sites in the root action zone soils (0–30 cm). There was also no significant difference in GRSP-C/N between the two mangrove forest types in the non-root action zone soils (30–100 cm). However, the GRSP-C/N level in the mangroves was significantly lower than

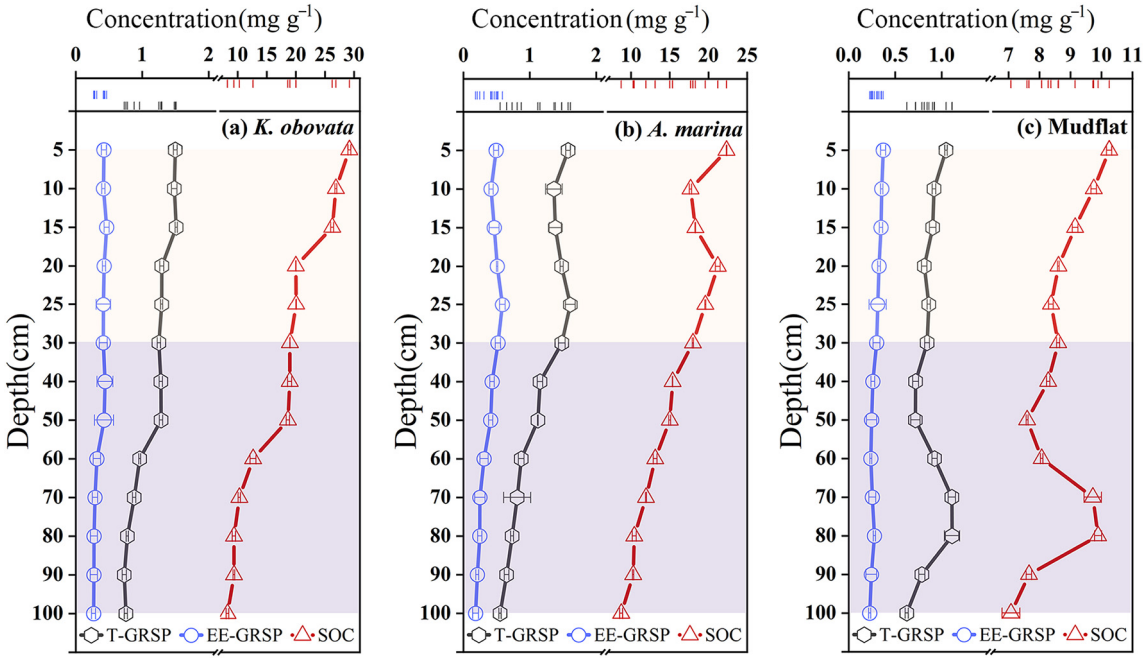

Fig. 2. Variation trends of T-GRSP, EE-GRSP, and SOC concentration in the 0–100 cm soil layer at three sampling sites. (a) *K. obovata* mangrove forest; (b) *A. marina* mangrove forest; (c) mudflat.

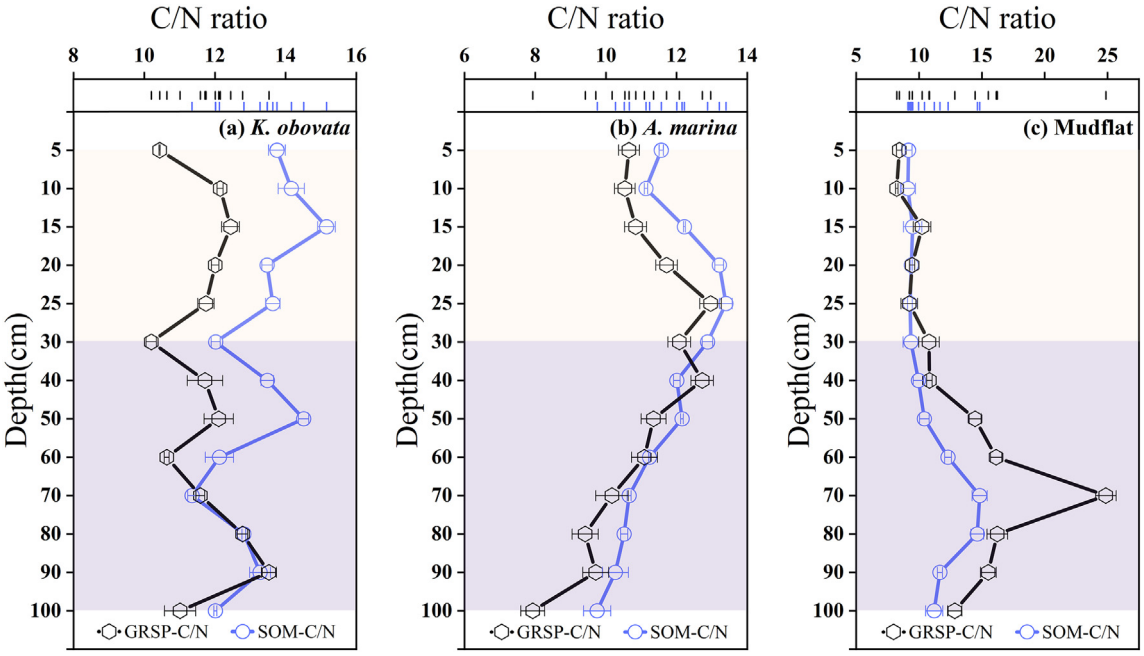

Fig. 3. Variation trends of SOM-C/N and GRSP-C/N in the 0–100 cm soil layer at three sampling sites. (a) *K. obovata* mangrove forest; (b) *A. marina* mangrove forest; (c) mudflat.

that in the mudflat for the non-root action zone soils (30–100 cm) ($p < 0.05$) (Fig. 3).

3.3. Chemical composition of GRSP

ATR-FTIR analysis was used to characterize the chemical composition of the GRSP and its variation during the burial process (Fig. 4). According to the commonly used classification, GRSP's composition was divided into four categories (Table S1): hydrocarbons (band I, II), proteins (bands III, IV, and V), polysaccharides (band VI), and nucleic acids (band VII). The hydrocarbon components in GRSP accounted for the largest proportion (~50%), followed by the protein (~30%), polysaccharide (~10%), and nucleic acid components (~4%). Compared with the GRSP in the surface layer, the GRSP in the bottom layer contained higher proportions of hydrocarbon components at all sites. In contrast, the proportions of protein and nucleic acid components in the bottom layer were lower than those in the surface layer. Moreover, the proportion of GRSP's polysaccharide component in the bottom layer of the mudflat soil was lower than that in the surface layer. However, the opposite trend for this component was found in the two mangrove forest soils (Fig. 4).

It is notable that mangrove forests have high deposition rates. To further clarify the characteristics of the variation in GRSP chemical composition

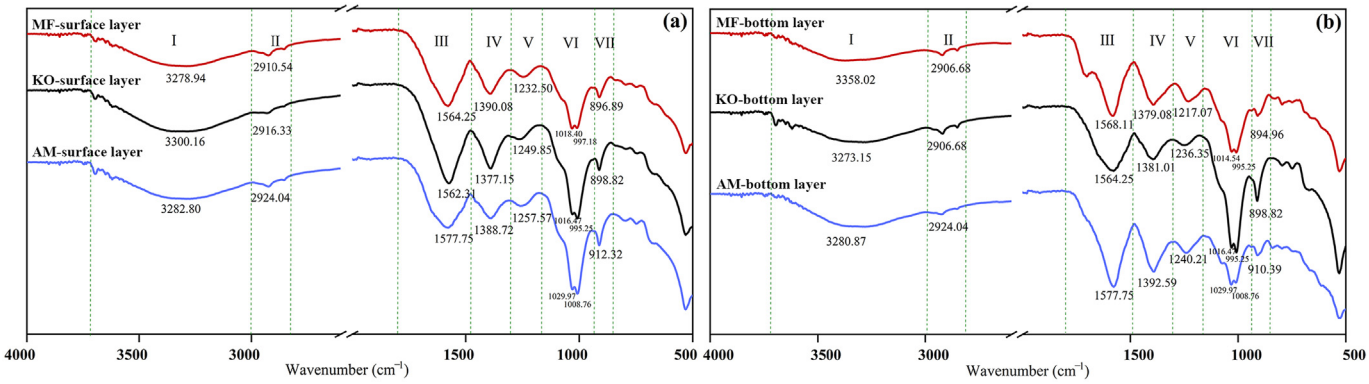

	Chemical composition(%)	Hydrocarbons (I+II)	Proteins (III+IV+V)	Polysaccharides (VI)	Nucleic acids (VII)
(a)	MF-surface layer	50.90	33.71	10.96	4.43
	KO-surface layer	51.36	33.76	10.54	4.33
	AM-surface layer	51.04	34.36	10.31	4.30
(b)	MF-bottom layer	53.05	33.28	9.52	4.15
	KO-bottom layer	52.01	33.62	11.06	3.31
	AM-bottom layer	52.65	31.96	11.83	3.55

Fig. 4. FTIR spectra of GRSP and the relative concentration of GRSP's chemical components (hydrocarbons, proteins, polysaccharides, and nucleic acids) in the three sample sites surface layer and bottom layer soils. MF, KO, and AM represent the soils of mudflat, *K. obovata* mangrove forest, and *A. marina* mangrove forest, respectively; (a) FTIR spectra of GRSP in the surface layer soil (5 cm) of three sample sites and the corresponding relative concentration of GRSP's chemical components; (b) FTIR spectra of GRSP in the bottom layer soil (100 cm) of three sample sites and the corresponding relative concentration of GRSP's chemical components.

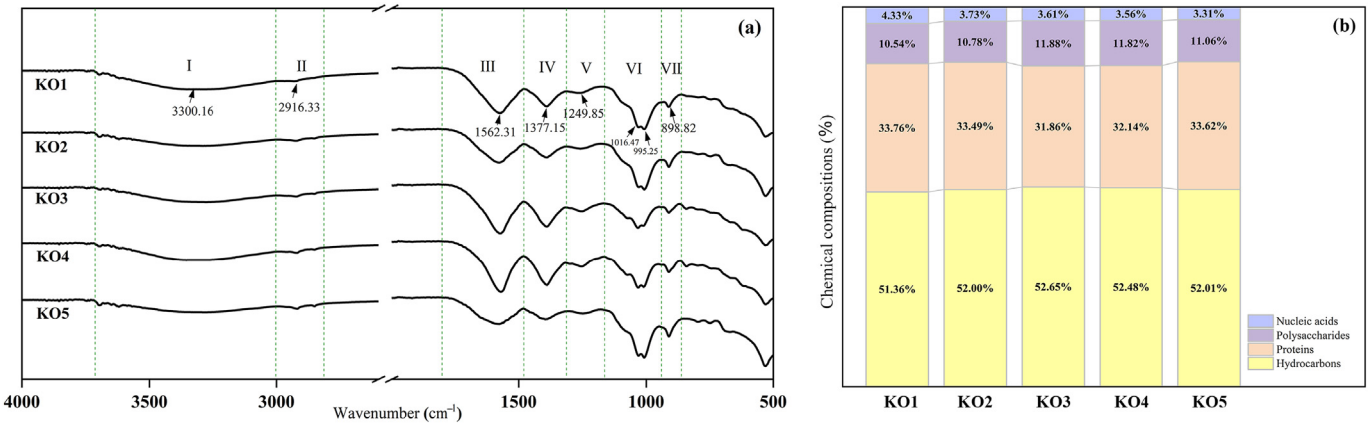

Fig. 5. FTIR spectra and the relative concentration of GRSP's chemical compositions (hydrocarbons, proteins, polysaccharides, and nucleic acids) in *K. obovata* mangrove forest soil. (a) FTIR spectra of GRSP; (b) the relative concentration of GRSP's chemical compositions. KO-num cm represents the soil depth of *K. obovata* mangrove forest.

during the burial process, the ATR-FTIR spectra of GRSP in the *K. obovata* mangrove forest soils were analyzed (Fig. 5a). As burial depth increased, the four GRSP components changed as follows: the proportion of nucleic acids continued to decrease, while the proportion of proteins initially decreased and then increased with a valley value (31.86%) detected at a depth of 50–60 cm; the proportion of hydrocarbons and polysaccharides increased and subsequently decreased, and the peak values (52.65% and 11.88% respectively) appeared at a depth of 50–60 cm (Fig. 5b).

3.4. GRSP stability index

The *K. obovata* mangrove forest soil samples collected at depths of 5, 30, 60, 90, and 100 cm were used to determine the recalcitrance index (RI) and the enrichment factor of GRSP to characterize trends in its stability with increasing burial depth.

Analysis of the SS ^{13}C NMR data showed that GRSP mainly consisted of O-alkyl C, alkyl C, and carboxyl C. The proportion of carboxyl C was the highest (32.77% ± 5.50%), followed by alkyl C (30.56% ± 8.34%) and O-alkyl C (24.35% ± 5.29%), while the proportion of aromatic carbon was the lowest (12.32% ± 3.14%). The proportions of carbon components in the GRSP varied with depth (Fig. 6). As burial depth increased, the carboxyl C (−17.08%) and O-alkyl C (−9.88%) proportions in GRSP decreased, while the proportions of alkyl C (+24.88%) and aromatic C (+2.08%) increased. The recalcitrance index shows a negative exponential trend with increasing depth. At a depth of 50 cm, the recalcitrance index reached a maximum (0.99 ± 0.04), and then tended to stabilize (Fig. 6).

Linear fitting was performed with burial as the horizontal coordinate and the GRSP's enrichment factor as the vertical coordinate. It was found that the GRSP/SOC ratio showed a linear increase with increasing depth (Fig. 7).

4. Discussion

4.1. Influence of habitat heterogeneity on GRSP concentration and chemical composition

The results show that the concentration of GRSP in mangrove forest soil was significantly higher than that in mudflat soil (Fig. 2), and this was more obvious in the root action zone (0–30 cm). This is consistent with the results of a study conducted in the Sundarban mangrove forest (Das et al., 2020). There are known to be two sources of GRSP in coastal wetlands: terrestrial and endogenous GRSP (Adame et al., 2010). The endogenous GRSP produced by AMF in mangrove roots and terrestrial GRSP intercepted by mangrove roots (Hien et al., 2018) are responsible for the higher GRSP

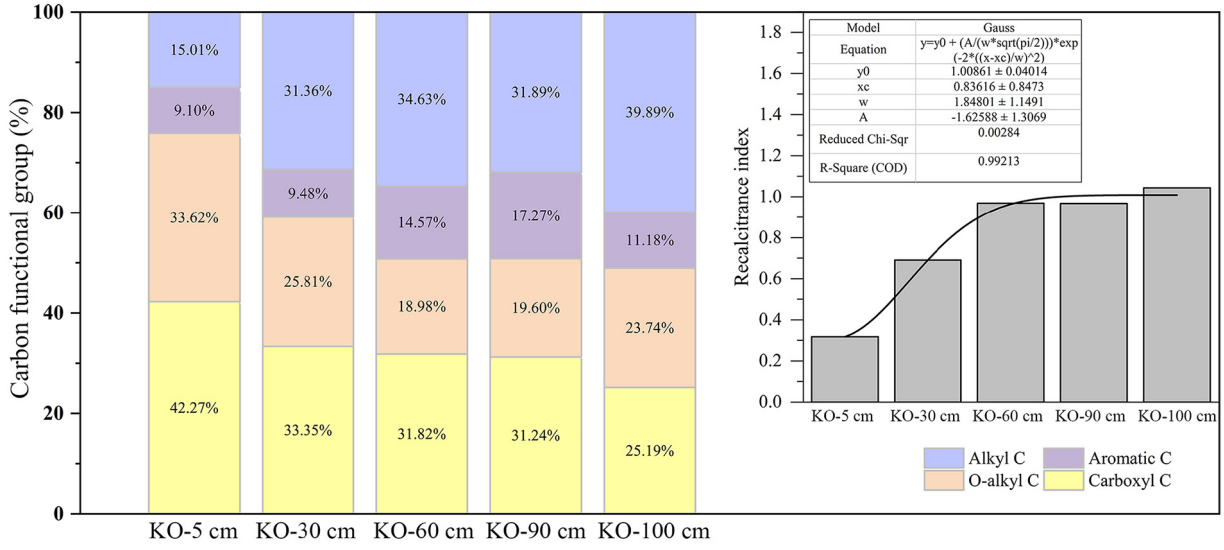

Fig. 6. Distributions of functional groups and the recalcitrance indexes of GRSP in the *K. obovata* mangrove forest soils. The inserted figures present the recalcitrance indexes (RI), indicated by (alkyl C + aromatic C)/(O-alkyl C + carboxyl C) of GRSP. With the burial depth as the horizontal coordinate and the RI value of GRSP as the vertical coordinate, the bar chart was plotted and then fitted with an exponential function. KO-num cm represents the soil depth of *K. obovata* mangrove forest.

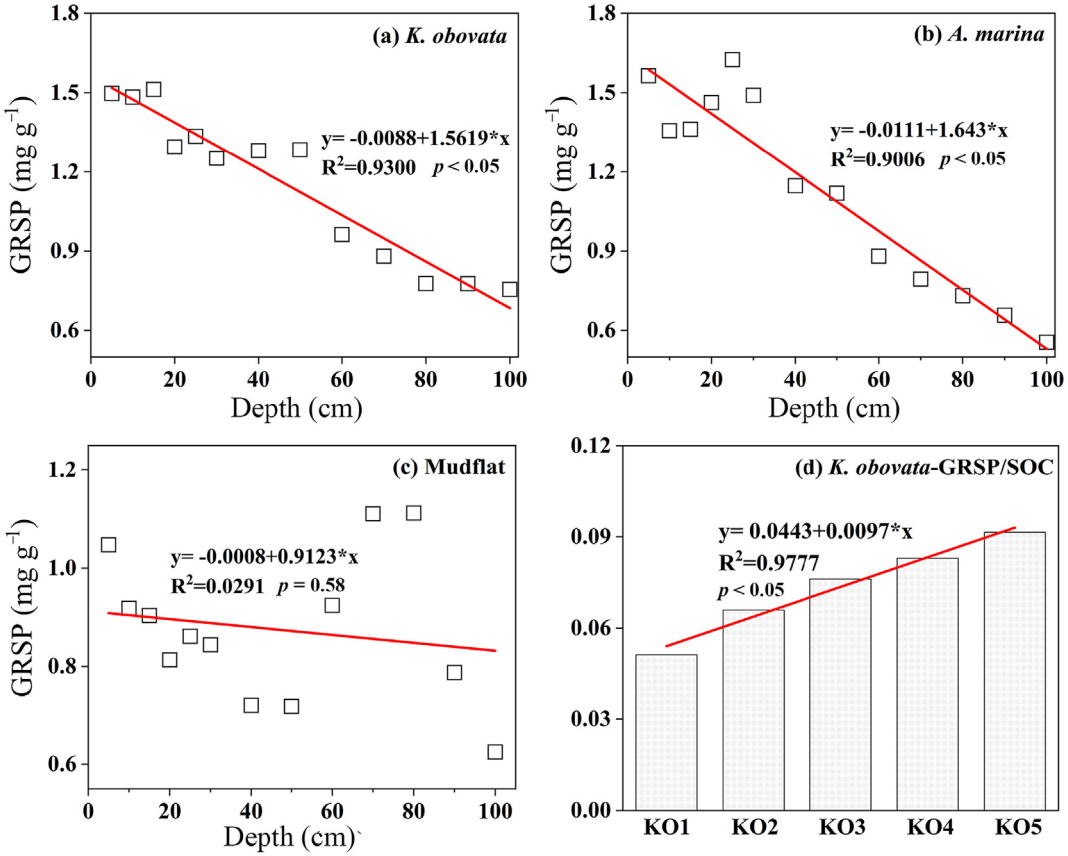

Fig. 7. Linear regression results of T-GRSP concentration in soils from three sampling sites and the variation trend of GRSP/SOC ratio with increasing depth. The first three figures show the linear relationship between GRSP concentration and burial depth in *K. obovata* mangrove forest (a), *A. marina* mangrove forest (b), and mudflat (c); (d) KO-num cm represents the soil depth of *K. obovata* mangrove forest.

concentration in mangrove compared to mudflat. Moreover, high salinity has an inhibitory effect on the growth and colonization of the AMF mycelium (Guo and Gong, 2013; Krishnamoorthy et al., 2014; Guan et al., 2020). Sengupta and Chaudhuri (2002) found a significant negative correlation between soil salinity and rate of AMF colonization in Ganges estuary mangroves, and studies of the Sundarbans in India (Kumar and Ghose, 2008) and five mangroves in southern China (Hu et al., 2015) reached the same conclusion. Therefore, the decrease in AMF colonization rate due to higher salinity may be the reason for the lower GRSP concentration in *A. marina* mangrove forest soil compared to *K. obovata*.

EE-GRSP is newly generated by AMF and is considered to be a labile component of T-GRSP (Koide and Peoples, 2013; Wu et al., 2014a; Liu et al., 2021). However, the rate of degradation of EE-GRSP was smaller than that of T-GRSP in this study. The results of field experiments reported by Wu et al. (2014b) also support this finding, which may imply that EE-GRSP is a less easily degradable fraction of T-GRSP. In addition, T-GRSP concentration from the three sampling sites decreased with increasing depth (Fig. 7). This is consistent with results previously reported in the Bay of Bengal, India (Das et al., 2020). Notably, the degradation rate of T-GRSP was significantly higher in mangrove forest soils than in mudflat soils, indicating that long-term flooding may provide a more ideal anaerobic storage environment for GRSP (Kaal et al., 2020).

The C/N ratio is an indicator of differences in soil composition and the structure of organic matter (Kerambrun and Guerin, 1993; Ito et al., 2014; Chmolowska et al., 2016; Kramer et al., 2017). In the non-root action zone (30–100 cm), the value of GRSP-C/N for mangrove forest soil was significantly lower than that of mudflat soil. Differences in GRSP-C/N between mangrove and mudflat soil suggest that there is a difference in chemical composition between the GRSP samples in these habitats. The same conclusion can be drawn from the analysis of the FTIR data. The proportion of GRSP polysaccharides in mangrove soils tended to increase with increasing burial depth, while the opposite trend was the case in mudflat soils (Fig. 4). Moreover, there was a positive correlation between SOM-C/N and GRSP-C/N in all sites (Table S3). Other studies have obtained findings consistent with ours (Bai et al., 2009; Fokom et al., 2012; Gomes et al., 2021) and further demonstrate the substantial contribution of GRSP to SOM. Therefore, it is reasonable to consider GRSP as a factor in SOM heterogeneity. Given that the purification method does not completely remove humic substances and other SOM fractions from GRSP (Holátko et al., 2021), this may account for the positive correlation between GRSP-C/N and SOM-C/N.

4.2. Effect of burial processes on the chemical composition of GRSP in mangroves

The decrease in GRSP concentration with increasing depth has been frequently reported (Wang et al., 2018; Kaal et al., 2020). However, only a limited number of studies of the GRSP's chemical composition have been conducted, and even fewer have considered its dynamic changes (Wang et al., 2020; Zhang et al., 2017). We have calculated the absolute values and degradation rates of GRSP's four component types (Table 1). The absolute values of these components all decreased with increasing depth, which is an inevitable result of the decrease with depth of the GRSP's concentration (Fig. 2). Interestingly, the variation in the relative values of the four components depends largely on differences in their degradation rates, with differences more obvious at depths below 60 cm. The degradation rate of the hydrocarbon fraction decreased significantly in depths below 60 cm, and the protein fraction even showed a negative value. In contrast, the degradation rates of both the nucleic acid and polysaccharide fractions showed an increasing trend. These trends led to the increases in the proportions of hydrocarbon and protein fractions as well as the decreases in nucleic acid and polysaccharide at greater depth. The factors affecting the

Table 1
Absolute values and degradation rates of the four compositions in GRSP.

Depth (cm)	GRSPs (mg g^{-1})	Hydrocarbons			Proteins			Polysaccharides			Nucleic acids		
		Absolute value	Degradation rate (per stage)	Total degradation rate	Absolute value	Degradation rate (per stage)	Total degradation rate	Absolute value	Degradation rate (per stage)	Total degradation rate	Absolute value	Degradation rate (per stage)	Total degradation rate
5	33.50 ± 0.07	17.21	–	–	11.31	–	–	3.53	–	–	1.45	–	–
30	12.00 ± 0.13	6.24	63.73%	63.73%	4.02	64.46%	64.46%	1.29	63.46%	63.46%	0.45	68.97%	68.97%
60	7.10 ± 0.04	3.74	40.10%	78.27%	2.26	43.78%	80.02%	0.84	34.88%	76.20%	0.26	42.22%	82.07%
90	6.57 ± 0.02	3.45	7.75%	79.95%	2.11	6.64%	81.34%	0.78	7.14%	77.90%	0.23	8.90%	83.89%
100	6.37 ± 0.09	3.31	4.06%	80.76%	2.14	−1.42%	81.08%	0.70	10.26%	80.17%	0.21	9.76%	85.52%

Note: GRSPs refer to the dry weight of purified T-GRSP. The absolute values were calculated as the product of the GRSPs and the relative values of the GRSP's compositions measured by FTIR. Degradation rate (per stage) refers to the percentage reduction in the absolute value of GRSP's composition compared to the previous soil layer. Total degradation rate refers to the percentage reduction in absolute value of GRSP's composition compared to the surface layer (5 cm).

degradation rates of organic matter are complex and variable, and soil pH, microbial action, and the presence of protease and β-glucosidase enzymes are the driving forces in the mineralization of organic matter (Brown et al., 1994; Wu et al., 2014b). The pH of the *K. obovata* mangrove forest soil ranged from 5.50 to 7.66, tending to increase with depth (Table S4). Combined with the physicochemical properties of this soil, we investigated the factors that may affect the degradation of GRSP during the burial process.

Hydrocarbons are degraded primarily by bacteria and fungi in the soil (Cason et al., 2019; Leahy and Colwell, 1990). During this process, pH is the main factor influencing the degradation rate. The degradation rate of hydrocarbons generally increases as pH rises from 5.0 to 8.0, and reaches an optimal rate at a value of approximately 7.8 (Dibble and Bartha, 1979; Husain et al., 1997; Gennadiev et al., 2015). This contrasts with trends in the variation of GRSP hydrocarbon components found in this study, which may be attributed to the insignificant role of microorganisms in the deep soil layer. In addition, there was a significantly negative correlation between soil pH and the proportion of nucleic acids in the GRSP ($R^2 = -0.904$, $p < 0.05$). Hansen et al. (2016) found that elevated pH could promote the degradation of SOM, and the same conclusion was obtained in a study of the effect of pH on the degradation of nucleic acid fractions (Ivarson et al., 1982). The results of the present study reconfirmed the effect of pH in promoting the degradation of nucleic acid fractions.

Microorganisms are known to directly obtain organic nitrogen from the soil in the form of oligopeptides and amino acids (Kuzyakov and Xu, 2013; Philippot et al., 2013; Moreau et al., 2019). In addition, Greenfield et al. (2020) found that proteases could promote the decomposition of proteins in the root action zone. In the present study, it is hypothesized that the co-action of microorganisms and root surface proteases may be one of the reasons for the decrease in the protein components of GRSP. At depths of 0–30 cm, stronger microbial action and root action resulted in the rapid degradation of the protein fractions. As depth increased, the microbial metabolic activity declined and the role of the root system was weakened (Chaopricha and Marín-Spiotta, 2014), leading to a reduction in the rate of protein degradation. It is notable that microbial metabolic activity has an impact on the redox potential of soils (Guo et al., 2022). Several studies have used changes in redox potential to indicate microbial activity, which is simpler and less costly than other methods such as genome sequencing and electrochemistry (DeAngelis et al., 2010; Hunting and van der Geest, 2011; Kralova et al., 1992). Redox potential is a useful indicator to further characterize the effect of microorganisms on GRSP degradation.

Mangrove litter is rich in polysaccharides such as cellulose, hemicellulose, and pectin (Furusawa, 2019). Moreover, the mucous produced by mangrove plants roots is also rich in polysaccharides (Amicucci et al., 2019; Nazari, 2021). Both the litter and mangrove root exudates are possible sources of the polysaccharide component of GRSP, and they jointly promote the accumulation of polysaccharides within the root action zone. However, a variety of bacteria, including anaerobic bacteria, play a key role in the degradation of the carbohydrates (Priya et al., 2018). Microbial action is likely to be the dominant reason for the reduction in levels of the GRSP's polysaccharide component within the non-root action zone.

In summary, soil pH, microbial action and soil enzymes may be key factors affecting the degradation of GRSP. In addition, tide scouring, animal interference, and other physicochemical properties of the soil may also affect the chemical composition of GRSP during deposition. The complex and variable chemical composition of GRSP is likely to be responsible for its ability to perform a variety of ecological functions.

4.3. Effect of burial processes on the stability of GRSP

Several studies have shown that GRSP does not degrade easily in soil (Lovelock et al., 2004b; Fokom et al., 2012; Cissé et al., 2020). The stretching in the 3300 cm^{-1} and 898 cm^{-1} band show that GRSP contains a large number of aromatic compounds (Fig. 4 and 7a), which further demonstrates that GRSP is a refractory organic matter (Marín-Spiotta et al., 2014). At present, various methods used to evaluate the stability of GRSP are not uniform. In this study, two common methods were used to characterize the effect of burial process on the stability of GRSP in *K. obovata* mangrove forest soils.

4.3.1. Evaluation using the enrichment factor of GRSP

The enrichment factor analysis showed that the proportion of GRSP in the SOC increased linearly with increasing depth. This result is consistent with a long-term bare fallow trial reported by Cissé et al. (2020), who found that the enrichment factor of GRSP also showed an increasing trend over time in an undisturbed area. In other words, GRSP was more stable than the other components in SOM. It is inferred that the increasing contribution of GRSP to SOC during the deposition process may be common under natural environmental conditions. Therefore, the carbon sequestration potential of GRSP should not be underestimated.

4.3.2. Evaluation using the recalcitrance index (RI)

The RI is widely used to study the decomposition level of soil organic matter (SOM) and humus (Baldock and Preston, 1995; Larionova et al., 2015; Mathers et al., 2003). Presently, it is also used to determine the degree of GRSP decomposition. A previous study has shown that the RI of GRSP was higher than that of SOM in tropical forests (Zhang et al., 2017). In other words, GRSP is more difficult to degrade and has a higher carbon sequestration capacity than other fractions of SOM (Singh et al., 2020). In the present study, the RI of GRSP tended to increase with depth and stabilized at a depth of 50 cm (0.99 ± 0.04) (Fig. 6), suggesting that the stability of GRSP levelled off after a progressive increase. The analysis of data also revealed that the degradation rate of GRSP decreased with increasing depth (Table 1). This is probably due to the soil burial process acting as a 'sieve'. The easily degradable fractions of GRSP decreased with the increasing burial depth, while the less easily degradable fractions accumulated in the deeper soil layers. In addition, several studies have shown that the average retention time of organic carbons is longer in deeper soil layers than in surface layers (Baisden and Parfitt, 2007; Rumpel and Koegel-Knabner, 2011; Chaopricha and Marín-Spiotta, 2014). The degradation trend of GRSP in this study was consistent with that finding, indicating that the deep soil layers play an important role in the long-term sequestration of GRSP.

Overall, GRSP is a relatively stable component of organic matter in mangrove soils and its carbon sequestration potential cannot be ignored. The stability of GRSP increased with increasing burial depth until constant at depths of 50 cm and below. In this process, the deep soil layers served as a storage site for the stable fractions of GRSP.

5. Conclusions

In conclusion, the results show that both the concentration and chemical composition of GRSP were habitat-heterogeneous. The GRSP concentration in mangrove forest soils was higher than that in mudflat. The proportion of the polysaccharide compositions of GRSP in mangrove forest soils increased with increasing depth, while the opposite trend was observed in the mudflat. In addition, GRSP concentration decreased with increasing burial depth and there were differences in the degradation rates of the GRSP components. The degradation rates of the hydrocarbon and protein fractions continued to decrease at depths from 50 to 100 cm of the soil, while those of the polysaccharide and nucleic acid fractions continued to increased. Microbial action, pH, and salinity appear to be the main factors affecting the GRSP's concentration and composition. A limitation of this study is that the action mechanisms of the causal factors are unclear and need to be further explored. Additionally, it seems that the deep soil layers are more conducive for GRSP sequestration. These findings enhance our understanding of the compositional characteristics and storage mechanisms of GRSP. However, the effects of GRSP heterogeneity on eco-environmental functions such as soil aggregate formation and heavy metal adsorption require further investigation.

CRediT authorship contribution statement

Zhenli Guo: Methodology, Conceptualization, Validation, Formal analysis, Investigation, Data curation, Writing - original draft, Writing - review & editing.

Jingchun Liu: Methodology, Conceptualization, Writing - original draft, Writing - review & editing, Supervision.

Jiajia Wu: Investigation, Validation.

Dan Yang: Resources, Investigation, Formal analysis, Writing - review & editing.

Kang Mei: Resources, Investigation, Formal analysis, Writing - review & editing.

Hanyi Li: Investigation, Resources.

Haoliang Lu and **Chongling Yan:** Resources, Investigation, Formal analysis, Funding acquisition.

Declaration of competing interest

The authors declare that they have no known competing financial interests or personal relationships that could have appeared to influence the work reported in this paper.

Acknowledgments

The authors would like to acknowledge the editor and anonymous reviewers whose comments and advice greatly improved the quality of this paper. This research was kindly supported and funded by the Ministry of Science and Technology of the People's Republic of China (2018YFC1406603), and the National Natural Science Foundation of China (42076168). We would like to thank Le He for dedicating work to the experiments. We also would like to thank Enago (www.enago.cn) providing language help. Special thanks to Tan Kah Kee Innovation Laboratory of Xiamen University for instrumentation support.

Appendix A. Supplementary data

Supplementary data to this article can be found online at https://doi.org/10.1016/j.scitotenv.2022.155351.

References

Adame, M.F., Neil, D., Wright, S.F., Lovelock, C.E., 2010. Sedimentation within and among mangrove forests along a gradient of geomorphological settings. Estuar. Coast. Shelf Sci. 86, 21–30. https://doi.org/10.1016/j.ecss.2009.10.013.

Adame, M.F., Wright, S.F., Grinham, A., Lobb, K., Reymond, C.E., Lovelock, C.E., 2012. Terrestrial-marine connectivity: patterns of terrestrial soil carbon deposition in coastal sediments determined by analysis of glomalin related soil proteinJ. Limnol. Oceanogr. 57, 1492–1502. https://doi.org/10.4319/lo.2012.57.5.1492.

Amicucci, M.J., Galermo, A.G., Guerrero, A., Treves, G., Nandita, E., Kailemia, M.J., Higdon, S.M., Pozzo, T., Labavitch, J.M., Bennett, A.B., Lebrilla, C.B., 2019. Strategy for structural elucidation of polysaccharides: elucidation of a maize mucilage that harbors diazotrophic bacteria.J. Anal. Chem. 91, 7254–7265. https://doi.org/10.1021/acs.analchem.9b00789.

Bai, C., He, X., Tang, H., Shan, B., Zhao, L., 2009. Spatial distribution of arbuscular mycorrhizal fungi, glomalin and soil enzymes under the canopy of Astragalus adsurgens Pall. In the Mu Us sandlandChina. J. Soil Biol. Biochem. 41, 941–947. https://doi.org/10.1016/J.SOILBIO.2009.02.010.

Baisden, W.T., Parfitt, R.L., 2007. Bomb C-14 enrichment indicates decadal C pool in deep soil?J. Biogeochemistry 85, 59–68. https://doi.org/10.1007/s10533-007-9101-7.

Baldock, J.A., Preston, C.M., 1995. Chemistry of carbon decomposition processes in forests as revealed by solid-state carbon-13 nuclear magnetic resonance. In: McFee, W.W., Kelly, J.M. (Eds.), Carbon Forms and Functions in Forest Soils. E-Publishing Inc., Florida, pp. 89–117 https://doi.org/10.2136/1995.carbonforms.c6.

Baldock, J.A., Oades, J.M., Waters, A.G., Peng, X., Vassallo, A.M., Wilson, M.A., 1992. Aspects of the chemical structure of soil organic materials as revealed by solid-state13C NMR spectroscopyJ. Biogeochemistry 16, 1–42. https://doi.org/10.1007/BF02402261.

Barea, J.M., Pozo, M.J., Aroca, R., Ferrol, N., Azcon, R., Lopez–Raez, J.A., Ruiz–Lozano, J.M., Azcon–Aguilar, C., 2014. Arbuscular mycorrhizas and their significance in promoting soil-plant system sustainability against environmental stresses. In: Gonzalez, M.B.R., GonzalezLopez, J. (Eds.), Beneficial Plant-Microbial Interactions: Ecology and Applications, pp. 353–387.

Brown, B.A., Hayes, R.M., Tyler, D.D., Mueller, T.C., 1994. Effect of tillage and cover crop on fluometuron adsorption and degradation under controlled conditionsJ. Weed Sci. 42, 629–634. https://doi.org/10.1017/S0043174500077067.

Cason, E.D., Vermeulen, J.G., Müller, W.J., van Heerden, E., Valverde, A., 2019. Aerobic and anaerobic enrichment cultures highlight the pivotal role of facultative anaerobes in soil hydrocarbon degradationJ. J. Environ. Sci. Health A Tox. Hazard. Subst. Environ. Eng. 54, 408–415. https://doi.org/10.1080/10934529.2018.1558902.

Chaopricha, N.T., Marín-Spiotta, E., 2014. Soil burial contributes to deep soil organic carbon storage.J. Soil Biol. Biochem. 69, 251–264. https://doi.org/10.1016/j.soilbio.2013.11.011.

Chen, S., Zhou, Z., Tsang, D.C.W., Wang, J., Odinga, E.S., Gao, Y., 2020. Glomalin-related soil protein reduces the sorption of polycyclic aromatic hydrocarbons by soilsJ. Chemosphere 260. https://doi.org/10.1016/j.chemosphere.2020.127603.

Chmolowska, D., Kozak, M., Laskowski, R., 2016. Soil physicochemical properties and floristic composition of two ecosystems differing in plant diversity: fallows and meadowsJ. Plant Soil 402, 317–329. https://doi.org/10.1007/S11104-015-2788-7/MEDIAOBJECTS/11104_2015_ 2788_MOESM2_ESM.DOC.

Cissé, G., van Oort, F., Chenu, C., Essi, M., Staunton, S., 2020. Is the operationally defined fraction of soil organic matter, "GRSP" (glomalin-related soil protein), stable in soils? Evidence from trends in long-term bare fallow soilJ. Eur. J. Soil Sci. 72, 1101–1112. https://doi.org/10.1111/ejss.12974.

Das, S., Ganguly, D., Chakraborty, S., Mukherjee, A., De, T.K., 2020. The first report of glomalin from the sundarban mangrove biosphere reserve, India, a long-term sediment carbon storageJ. Reg. Stud. Mar. Sci. 39. https://doi.org/10.1016/j.rsma.2020.101398.

DeAngelis, K.M., Silver, W.L., Thompson, A.W., Firestone, M.K., 2010. Microbial communities acclimate to recurring changes in soil redox potential statusJ. Environ. Microbiol. 12, 3137–3149. https://doi.org/10.1111/J.1462-2920.2010.02286.X.

Dibble, J.T., Bartha, R., 1979. Effect of environmental parameters on the biodegradation of oil sludgeJ. Appl. Environ. Microbiol. 37, 729–739. https://doi.org/10.1128/AEM.37.4.729-739.1979.

Driver, J.D., Holben, W.E., Rillig, M.C., 2005. Characterization of glomalin as a hyphal wall component of arbuscular mycorrhizal fungiJ. Soil Biol. Biochem. 37, 101–106. https://doi.org/10.1016/j.soilbio.2004.06.011.

Feng, J., Zhou, J., Wang, L., Cui, X., Ning, C., Wu, H., Zhu, X., Lin, G., 2017. Effects of short-term invasion of Spartina alterniflora and the subsequent restoration of native mangroves on the soil organic carbon, nitrogen and phosphorus stockJ. Chemosphere 184, 774–783. https://doi.org/10.1016/j.chemosphere.2017.06.060.

Fokom, R., Adamou, S., Teugwa, M.C., Boyogueno, A.D.B., Nana, W.L., Ngonkeu, M.E.L., Tchameni, N.S., Nwaga, D., Ndzomo, G.T., Zollo, P.H.A., 2012. Glomalin related soil protein, carbon, nitrogen, and soil aggregate stability as affected by land use variation in the humid forest zone of South CameroonJ. Soil Tillage Res. 120, 69–75. https://doi.org/10.1016/j.still.2011.11.004.

Furusawa, G., 2019. Biodiversity of plant polysaccharide-degrading bacteria in mangrove ecosystemJ. Trop. Life Sci. Res. 30, 157–172. https://doi.org/10.21315/tlsr2019.30.3.11.

Gennadiev, A.N., Pikovskii, Y.I., Tsibart, A.S., Smirnova, M.A., 2015. Hydrocarbons in soils: origin, composition, and behavior (Review)J. Eurasian Soil Sci. 48, 1076–1089. https://doi.org/10.1134/S1064229315100026.

Gillespie, A.W., Farrell, R.E., Walley, F.L., Ross, A.R.S., Leinweber, P., Eckhardt, K.U., Regier, T.Z., Blyth, R.I.R., 2011. Glomalin-related soil protein contains non-mycorrhizal-related heat-stable proteins, lipids, and humic materialsJ. Soil Biol. Biochem. 43, 766–777. https://doi.org/10.1016/j.soilbio.2010.12.010.

Gomes, V.M., Assis, I.R., Hobbs, R.J., Fernandes, G.W., 2021. Glomalin-related soil protein reflects the heterogeneity of substrate and vegetation in the campo rupestre ecosystemJ. J. Soil Sci. Plant Nutr. 21, 733–743. https://doi.org/10.1007/S42729-020-00396-7/FIGURES/3.

Greenfield, L.M., Hill, P.W., Paterson, E., Baggs, E.M., Jones, D.L., 2020. Do plants use root-derived proteases to promote the uptake of soil organic nitrogen?J. Plant and Soil 456, 355–367. https://doi.org/10.1007/s11104-020-04719-6.

Guan, B., Zhang, H., Wang, X., Yang, S., Chen, M., Hou, A., Cagle, G.A., Han, G., 2020. Salt is a main factor shaping community composition of arbuscular mycorrhizal fungi along a vegetation successional series in the Yellow River DeltaJ. CATENA 185, 104318. https://doi.org/10.1016/J.CATENA.2019.104318.

Guo, X., Gong, J., 2013. Differential effects of abiotic factors and host plant traits on diversity and community composition of root-colonizing arbuscular mycorrhizal fungi in a salt-stressed ecosystem. J. Mycorrhiza 2 (24), 79–94. https://doi.org/10.1007/S00572-013-0516-9 2013 24.

Guo, K., Song, Z., Wang, G., Tang, C., 2022. Detecting redox potentials using porous boron Nitride/ATP-DNA Aptamer/Methylene blue biosensor to monitor microbial activitiesJ. Micromachines 13, 83. https://doi.org/10.3390/MI13010083.

Hansen, M., Saarsalmi, A., Peltre, C., 2016. Changes in SOM composition and stability to microbial degradation over time in response to wood chip ash fertilisationJ. Soil Biol. Biochem. 99, 179–186. https://doi.org/10.1016/J.SOILBIO.2016.05.012.

He, J.D., Chi, G.G., Zou, Y.N., Shu, B., Wu, Q.S., Srivastava, A.K., Kuča, K., 2020. Contribution of glomalin-related soil proteins to soil organic carbon in trifoliate orange.J. Appl. Soil Ecol. 154. https://doi.org/10.1016/j.apsoil.2020.103592.

Hien, H.T., Marchand, C., Aime, J., Dang Hoai, N., Phan Nguyen, H., Nguyen Xuan, T., Nguyen Thi Kim, C., 2018. Belowground carbon sequestration in a mature planted mangroves (Northern Viet Nam). J. For. Ecol. Manag. 407, 191–199. https://doi.org/10.1016/j.foreco.2017.06.057.

Holátko, J., Brtnický, M., Kučerík, J., Kotianová, M., Elbl, J., Kintl, A., Kynický, J., Benada, O., Datta, R., Jansa, J., 2021. Glomalin - truths, myths, and the future of this elusive soil glycoproteinJ. Soil Biol. Biochem. 153. https://doi.org/10.1016/j.soilbio.2020.108116.

Hu, W.H., Wu, Y., Xin, G.R., Wang, Y.T., Guo, J.H., Peng, X., 2015. Arbuscular mycorrhizal fungi and their influencing factors for aegiceras corniculatuni and acanthus ilicifolius in southern ChinaJ. Pak. J. Bot. 47, 1581–1586.

Hunting, E.R., van der Geest, H.G., 2011. Predictability of bacterial activity and denitrification in aquatic sediments with continuous measurements of redox potentialJ. Int. J. Environ. Sci. Technol. 8:3 8, 553–560. https://doi.org/10.1007/BF03326241.

Husain, D.R., Goutx, M., Acquaviva, M., Gilewicz, M., Bertrand, J.C., 1997. The effect of temperature on eicosane substrate uptake modes by a marine bacterium Pseudomonas nautica strain 617: relationship with the biochemical content of cells and supernatantsJ. World J. Microbiol. Biotechnol. 13, 587–590. https://doi.org/10.1023/a:1018581829320.

Ito, E., Toriyama, J., Araki, M., Kiyono, Y., Kanzaki, M., Tith, B., Keth, S., Chandararity, L., Chann, S., 2014. Physicochemical surface-soil properties after litter-removal manipulation in a cambodian lowland dry evergreen forestJ. Jpn. Agric. Res. Q. 48, 195–211. https://doi.org/10.6090/jarq.48.195.

Ivarson, K.C., Schnitzer, M., Cortez, J., 1982. The biodegradability of nucleic acid bases adsorbed on inorganic and organic soil componentsJ. Plant Soil 64, 343–353. https://doi.org/10.1007/BF02372517.

Jia, X., Zhao, Y., Liu, T., Huang, S., Chang, Y., 2016. Elevated CO2 increases glomalin-related soil protein (GRSP) in the rhizosphere of Robinia pseudoacacia L. Seedlings in Pb- and Cd-contaminated soilsJ. Environ. Pollut. 218, 349–357. https://doi.org/10.1016/j.envpol.2016.07.010.

Kaal, J., Lavery, P.S., Martínez Cortizas, A., López-Costas, O., Buchaca, T., Salinas, C., Serrano, O., 2020. Reconstruction of 7500 years of coastal environmental change impacting seagrass ecosystem dynamics in oyster harbour (SW Australia)J. Palaeogeogr. Palaeoclimatol. Palaeoecol. 558, 109953. https://doi.org/10.1016/J.PALAEO.2020.109953.

Kerambrun, P., Guerin, J.P., 1993. Influence du Régime alimentaire Sur la composition chimique Elémentaire de Nebalia bipes (Crustacea, Leptostraca)J. Int. Rev. Ges. Hydrobiol. Hydrogr. 78, 151–159. https://doi.org/10.1002/IROH.19930780116.

Koide, R.T., Peoples, M.S., 2013. Behavior of Bradford-reactive substances is consistent with predictions for glomalinJ. Appl. Soil Ecol. 63, 8–14. https://doi.org/10.1016/J.APSOIL.2012.09.015.

Kothamasi, D., Kothamasi, S., Bhattacharyya, A., Kuhad, R.C., Babu, C.R., 2006. Arbuscular mycorrhizae and phosphate solubilising bacteria of the rhizosphere of the mangrove ecosystem of great nicobar island, IndiaJ. Biol. Fertil. Soils 42, 358–361. https://doi.org/10.1007/s00374-005-0035-8.

Kralova, M., Masscheleyn, P.H., Patrick, W.H., 1992. Redox potential as an indicator of electron availability for microbial activity and nitrogen transformations in aerobic soilJ. Zentralbl. Mikrobiol. 147, 388–399. https://doi.org/10.1016/S0232-4393(11)80348-3.

Kramer, M.G., Lajtha, K., Aufdenkampe, A.K., 2017. Depth trends of soil organic matter C:N and 15N natural abundance controlled by association with minerals. Biogeochemistry 136, 23–248. https://doi.org/10.1007/S10533-017-0378-X/MEDIAOBJECTS/10533_2017_378_ MOESM1_ ESM.PPTX.

Krishnamoorthy, R., Kim, K., Kim, C., Sa, T., 2014. Changes of arbuscular mycorrhizal traits and community structure with respect to soil salinity in a coastal reclamation landJ. Soil Biol. Biochem. 72, 1–10. https://doi.org/10.1016/J.SOILBIO.2014.01.017.

Kumar, T., Ghose, M., 2008. Status of arbuscular mycorrhizal fungi (AMF) in the Sundarbans of India in relation to tidal inundation and chemical properties of soilJ. Wetl. Ecol. Manag. 16, 471–483. https://doi.org/10.1007/S11273-008-9085-7/TABLES/6.

Kumar, S., Singh, A.K., Ghosh, P., 2018. Distribution of soil organic carbon and glomalin related soil protein in reclaimed coal mine-land chronosequence under tropical conditionJ. Sci. Total Environ. 625, 1341–1350. https://doi.org/10.1016/j.scitotenv.2018.01.061.

Kuzyakov, Y., Xu, X., 2013. Competition between roots and microorganisms for nitrogen: mechanisms and ecological relevanceJ. New Phytol. 198, 656–669. https://doi.org/10.1111/nph.12235.

Larionova, A.A., Zolotareva, B.N., Kolyagin, Y.G., Kvitkina, A.K., Kaganov, V.V., Kudeyarov, V.N., 2015. Composition of structural fragments and the mineralization rate of organic matter in zonal soilsJ. Eurasian Soil Sci. 48, 1110–1119. https://doi.org/10.1134/S1064229315100063.

Leahy, J.G., Colwell, R.R., 1990. Microbial degradation of hydrocarbons in the environmentJ. Microbiol. Rev. 54, 305–315. https://doi.org/10.1128/MR.54.3.305-315.1990.

Liu, H., Ren, H., Hui, D., Wang, W., Liao, B., Cao, Q., 2014. Carbon stocks and potential carbon storage in the mangrove forests of ChinaJ. J. Environ. Manag. 133, 86–93. https://doi.org/10.1016/j.jenvman.2013.11.037.

Liu, R.C., Gao, W.Q., Srivastava, A.K., Zou, Y.N., Kuča, K., Hashem, A., Wu, Q.S., Abd_Allah, E.F., 2021. Differential Effects of Exogenous Glomalin-Related Soil Proteins on Plant Growth of Trifoliate Orange Through Regulating Auxin Changes. J. Front. Plant Sci. 12, 1945. https://doi.org/10.3389/fpls.2021.745402.

Lovelock, C.E., Wright, S.F., Clark, D.A., Ruess, R.W., 2004a. Soil stocks of glomalin produced by arbuscular mycorrhizal fungi across a tropical rain forest landscapeJ. J. Ecol. 92, 278–287. https://doi.org/10.1111/j.0022-0477.2004.00855.x.

Lovelock, C.E., Wright, S.F., Nichols, K.A., 2004b. Using glomalin as an indicator for arbuscular mycorrhizal hyphal growth: an example from a tropical rain forest soilJ. Soil Biol. Biochem. 36, 1009–1012. https://doi.org/10.1016/j.soilbio.2004.02.010.

Marín-Spiotta, E., Chaopricha, N.T., Plante, A.F., Diefendorf, A.F., Mueller, C.W., Grandy, A.S., Mason, J.A., 2014. Long-term stabilization of deep soil carbon by fire and burial during early holocene climate changeJ. Nat. Geosci. 7, 428–432. https://doi.org/10.1038/ngeo2169.

Mathers, N.J., Xu, Z.H., Blumfield, T.J., Berners-Price, S.J., Saffigna, P.G., 2003. Composition and quality of harvest residues and soil organic matter under windrow residue management in young hoop pine plantations as revealed by solid-state C-13 NMR spectroscopyJ. For. Ecol. Manag. 175, 467–488. https://doi.org/10.1016/s0378-1127(02)00182-2.

Moreau, D., Bardgett, R.D., Finlay, R.D., Jones, D.L., Philippot, L., 2019. A plant perspective on nitrogen cycling in the rhizosphereJ. Funct. Ecol. 33, 540–552. https://doi.org/10.1111/1365-2435.13303.

Nazari, M., 2021. Plant mucilage components and their functions in the rhizosphereJ. Rhizosphere 18. https://doi.org/10.1016/j.rhisph.2021.100344.

Negrin, V.L., Spetter, C.V., Asteasuain, R.O., Perillo, G.M.E., Marcovecchio, J.E., 2011. Influence of flooding and vegetation on carbon, nitrogen, and phosphorus dynamics in the pore water of a Spartina alterniflora salt marshJ. J. Environ. Sci. 23, 212–221. https://doi.org/10.1016/S1001-0742(10)60395-6.

Ostertag, R., Marín-Spiotta, E., Silver, W.L., Schulten, J., 2008. Litterfall and decomposition in relation to soil carbon pools along a secondary forest chronosequence in Puerto RicoJ. Ecosystems 11, 701–714. https://doi.org/10.1007/s10021-008-9152-1.

Philippot, L., Raaijmakers, J.M., Lemanceau, P., van der Putten, W.H., 2013. Going back to the roots: the microbial ecology of the rhizosphereJ. Nat. Rev. Microbiol. 11, 789–799. https://doi.org/10.1038/nrmicro3109.

Priya, G., Lau, N.S., Furusawa, G., Dinesh, B., Foong, S.Y., Amirul, A.A.A., 2018. Metagenomic insights into the phylogenetic and functional profiles of soil microbiome from a managed mangrove in MalaysiaJ. Agri Gene 9, 5–15. https://doi.org/10.1016/j.aggene.2018.07.001.

Rillig, M.C., 2004. Arbuscular mycorrhizae, glomalin, and soil aggregationJ. Can. J. Soil Sci. 84, 355–363. https://doi.org/10.4141/S04-003.

Rillig, M.C., Wright, S.F., Nichols, K.A., Schmidt, W.F., Torn, M.S., 2001. Large contribution of arbuscular mycorrhizal fungi to soil carbon pools in tropical forest soilsJ. Plant Soil 233, 167–177. https://doi.org/10.1023/A:1010364221169.

Rosier, C.L., Piotrowski, J.S., Hoye, A.T., Rillig, M.C., 2008. Intraradical protein and glomalin as a tool for quantifying arbuscular mycorrhizal root colonizationJ. Pedobiologia 52, 41–50. https://doi.org/10.1016/j.pedobi.2008.02.002.

Rumpel, C., Koegel-Knabner, I., 2011. Deep soil organic matter-a key but poorly understood component of terrestrial C cycleJ. Plant Soil 338, 143–158. https://doi.org/10.1007/s11104-010-0391-5.

Schindler, F.v., Mercer, E.J., Rice, J.A., 2007. Chemical characteristics of glomalin-related soil protein (GRSP) extracted from soils of varying organic matter content. J. Soil Biol. Biochem. 39, 320–329. https://doi.org/10.1016/j.soilbio.2006.08.017.

Sengupta, A., Chaudhuri, S., 2002. Arbuscular mycorrhizal relations of mangrove plant community at the Ganges river estuary in India. J. Mycorrhiza 4 (12), 169–174. https://doi.org/10.1007/S00572-002-0164-Y 2002 12.

Silva, C.A.R., Oliveira, S.R., Rego, R.D.P., Mozeto, A.A., 2007. Dynamics of phosphorus and nitrogen through litter fall and decomposition in a tropical mangrove forestJ. Mar. Environ. Res. 64, 524–534. https://doi.org/10.1016/j.marenvres.2007.04.007.

Singh, A.K., Rai, A., Singh, N., 2016. Effect of long term land use systems on fractions of glomalin and soil organic carbon in the indo-gangetic plainJ. Geoderma 277, 41–50. https://doi.org/10.1016/j.geoderma.2016.05.004.

Singh, A.K., Rai, A., Pandey, V., Singh, N., 2017. Contribution of glomalin to dissolve organic carbon under different land uses and seasonality in dry tropicsJ. J. Environ. Manag. 192, 142–149. https://doi.org/10.1016/j.jenvman.2017.01.041.

Singh, A.K., Zhu, X., Chen, C., Wu, J., Yang, B., Zakari, S., Jiang, X.J., Singh, N., Liu, W., 2020. The role of glomalin in mitigation of multiple soil degradation problems. J https://doi.org/10.1080/10643389.2020.1862561.

Staunton, S., Saby, N.P.A., Arrouays, D., Quiquampoix, H., 2020. Can soil properties and land use explain glomalin-related soil protein (GRSP) accumulation? A nationwide survey in FranceJ. Catena 193. https://doi.org/10.1016/j.catena.2020.104620.

Tian, Y., Yan, C., Wang, Q., Ma, W., Yang, D., Liu, J., Lu, H., 2020. Glomalin-related soil protein enriched in δ13C and δ15N excels at storing blue carbon in mangrove wetlandsJ. Sci. Total Environ. 732, 138327. https://doi.org/10.1016/j.scitotenv.2020.138327.

Treseder, K.K., Turner, K.M., Mack, M.C., 2007. Mycorrhizal responses to nitrogen fertilization in boreal ecosystems: potential consequences for soil carbon storageJ. Glob. Chang. Biol. 13, 78–88. https://doi.org/10.1111/j.1365-2486.2006.01279.x.

Vodnik, D., Grcman, H., Macek, I., van Elteren, J.T., Kovacevic, M., 2008. The contribution of glomalin-related soil protein to pb and zn sequestration in polluted soilJ. Sci. Total Environ. 392, 130–136. https://doi.org/10.1016/j.scitotenv.2007.11.016.

Wang, Q., Wu, Y., Wang, W., Zhong, Z., Pei, Z., Ren, J., Wang, H., Zu, Y., 2014. Spatial variations in concentration, compositions of glomalin related soil protein in poplar plantations in northeastern China, and possible relations with soil physicochemical propertiesJ. Sci. World J. 2014, 13. https://doi.org/10.1155/2014/160403.

Wang, Q., Lu, H., Chen, J., Hong, H., Liu, J., Li, J., Yan, C., 2018. Spatial distribution of glomalin-related soil protein and its relationship with sediment carbon sequestration across a mangrove forestJ. Sci. Total Environ. 613–614, 548–556. https://doi.org/10.1016/J.SCITOTENV.2017.09.140.

Wang, Y., Ji, C., Shi, Z., Yin, X., Liu, C., 2019. Spatial distribution of glomalin-related soil proteins in coniferous and broadleaf mixed temperate forestJ. Notulae Botanicae Horti Agrobotanici Cluj-Napoca 47, 1087–1093. https://doi.org/10.15835/nbha47411621.

Wang, Q., Chen, J., Chen, S., Qian, L., Yuan, B., Tian, Y., Wang, Y., Liu, J., Yan, C., Lu, H., 2020. Terrestrial-derived soil protein in coastal water: metal sequestration mechanism and ecological functionJ. J. Hazard. Mater. 386, 12. https://doi.org/10.1016/j.jhazmat.2019.121655.

Wright, S.F., Upadhyaya, A., 1998. A survey of soils for aggregate stability and glomalin, a glycoprotein produced by hyphae of arbuscular mycorrhizal fungiJ. Plant Soil 198, 97–107. https://doi.org/10.1023/a:1004347701584.

Wu, Q.S., He, X.H., Zou, Y.N., He, K.P., Sun, Y.H., Cao, M.Q., 2012. Spatial distribution of glomalin-related soil protein and its relationships with root mycorrhization, soil aggregates, carbohydrates, activity of protease and β-glucosidase in the rhizosphere of Citrus unshiuJ. Soil Biol. Biochem. 45, 181–183. https://doi.org/10.1016/j.soilbio.2011.10.002.

Wu, Q.S., Cao, M.Q., Zou, Y.N., He, X., 2014a. Direct and indirect effects of glomalin, mycorrhizal hyphae and roots on aggregate stability in rhizosphere of trifoliate orange. J. Sci. Rep. 2014 (4:1 4), 1–8. https://doi.org/10.1038/srep05823.

Wu, Z., McGrouther, K., Huang, J., Wu, P., Wu, W., Wang, H., 2014b. Decomposition and the contribution of glomalin-related soil protein (GRSP) in heavy metal sequestration: field experimentJ. Soil Biol. Biochem. 68, 283–290. https://doi.org/10.1016/j.soilbio.2013.10.010.

Xiao, L., Zhang, Yang, Li, P., Xu, G., Shi, P., Zhang, Yi, 2019. Effects of freeze-thaw cycles on aggregate-associated organic carbon and glomalin-related soil protein in natural-succession grassland and chinese pine forest on the loess plateauJ. Geoderma 334, 1–8. https://doi.org/10.1016/j.geoderma.2018.07.043.

Xu, C., Wong, V.N.L., Reef, R.E., 2021. Effect of inundation on greenhouse gas emissions from temperate coastal wetland soils with different vegetation types in southern AustraliaJ. Sci. Total Environ. 763. https://doi.org/10.1016/j.scitotenv.2020.142949.

Yang, W.bin, Yuan, C.S., Tong, C., Yang, P., Yang, L., Huang, B.Q., 2017. Diurnal variation of CO2, CH4, and N2O emission fluxes continuously monitored in-situ in three environmental habitats in a subtropical estuarine wetland. Mar. Pollut. Bull. 119, 289–298. https://doi.org/10.1016/j.marpolbul.2017.04.005.

Zhang, Y.H., Huang, G.M., Wang, W.Q., Chen, L.Z., Lin, G.H., 2012. Interactions between mangroves and exotic spartina in an anthropogenically disturbed estuary in southern ChinaJ. Ecology 93, 588–597. https://doi.org/10.1890/11-1302.1.

Zhang, X., Wu, X., Zhang, S., Xing, Y., Wang, R., Liang, W., 2014. Organic amendment effects on aggregate-associated organic C, microbial biomass C and glomalin in agricultural soilsJ. Catena 123, 188–194. https://doi.org/10.1016/j.catena.2014.08.011.

Zhang, J., Tang, X., He, X., Liu, J., 2015. Glomalin-related soil protein responses to elevated CO2 and nitrogen addition in a subtropical forest: potential consequences for soil carbon accumulationJ. Soil Biol. Biochem. 83, 142–149. https://doi.org/10.1016/j.soilbio.2015.01.023.

Zhang, J., Tang, X.L., Zhong, S.Y., Yin, G.C., Gao, Y.F., He, X.H., 2017. Recalcitrant carbon components in glomalin-related soil protein facilitate soil organic carbon preservation in tropical forestsJ. Sci. Rep. 7, 9. https://doi.org/10.1038/s41598-017-02486-6.

Zhu, R., Zheng, Z., Li, T., He, S., Zhang, X., Wang, Y., Liu, T., 2019. Effect of tea plantation age on the distribution of glomalin-related soil protein in soil water-stable aggregates in southwestern ChinaJ. Environ. Sci. Pollut. Res. 26, 1973–1982. https://doi.org/10.1007/s11356-018-3782-4.